

ESTIMATION OF SKIN SURFACE TEMPERATURE OF SPACE VEHICLES DURING THE WHOLE FLIGHT ENVELOP

S. R. Chaudhry*, N. U. Saqib*, F. Umar*

*Advanced Computing and Engineering Solutions (ACES) Pakistan

Keywords: *surface, temperature, transient, supersonic, insulation*

Abstract

Aerodynamic heating is an important aspect of high supersonic and hypersonic flight of launch vehicles and sounding rockets. Due to Aerodynamic drag at high Mach numbers, skin temperatures of these vehicles may reach around thousands of degrees Kelvin. The protection of payload and vehicle structural integrity is of prime importance at such high temperatures. Material selection of the skin and insulation for the payload can be carried out only when near accurate skin temperature are known over the surface of a launch vehicle or a rocket. Several methods are utilized during conceptual design phase to calculate the skin temperatures once the flight trajectory is known. This paper describes a method for calculation of transient surface temperatures at supersonic and hypersonic speeds using CFD. This method can rapidly calculate the temperature and the heating rate time histories for complete flight trajectories. Semi empirical theories can be used to develop the procedure for boundary layer temperature transition to the surface temperature. However more accuracy is attained if boundary layer temperature and other flowfield parameters are coming from CFD. The results have been found in good agreement with the telemetry data available for different rocket systems.

1 Nomenclature

α	Angle of attack (Deg/Rad)
B	Factor ^[2]
C_p	specific heat of air at const pressure (BTU/lb deg F)
C	Solar constant (0.1192 BTU/sqft-sec)

c	specific heat of material (BTU/lb deg F)
H	Enthalpy (BTU/lb)
H^*	Reference enthalpy (BTU/lb)
H_r	Recovery enthalpy (BTU/lb)
h	Coefficient of heat transfer
k	Recovery factor, thermal conductivity
Kn	Knudsen number
L	Characteristic length
M	Mach number
Nu	Nusselt number
Pr	Prandtl number
Re_∞	Reynolds number = $\frac{\rho_\infty V_\infty r}{\mu_\infty}$
T	Temperature of air (Rankin)
T_m	Mean Temperature (Rankin)
T_I	Initial Temperature (Rankin)
T_P	Potential Temperature, a fictitious value (Rankin) ^[2]
T_r	Recovery temperature (Rankin)
T_w	Temperature of the wall (Rankin)
T^*	Reference temperature deg (Rankin)
V	Velocity (ft/sec)
w	Specific weight of material (lb/cuft)
ϵ	Emmisivity
β	Full cone angle
γ	Coefficient of specific heats
μ	Coefficient of viscosity (lb sec/sqft)
μ_0	Coefficient of viscosity at sea level (lb sec/sqft)
ρ	Density of air (slugs/cuft)
ρ_0	Density of air at sea level (slugs/cuft)
τ	Thickness of the material (ft)
δ	Boundary layer thickness
G	Skin Factor = $c\tau w$
λ	Mean free molecular path in a gaseous medium

Subscripts

∞	Free stream conditions
w	wall conditions
r	reference conditions, or at a distance r

2 Introduction

Aerodynamic heating is an important aspect of high supersonic and hypersonic flight of launch vehicles and the sounding rockets. Practical experience with the Space Shuttle suggest that viscous and high temperature effects are very critical with regard to accurately assessing different flow phenomenon such as aero thermal heating, shock boundary layer interaction and separated flow.

The high value of drag at high Mach numbers results into high skin temperatures of the range of thousands of degrees Kelvin. Drag of the vehicle at any given instant in time on any specified trajectory is a function of

Now for the accurate prediction of temperature and lot many other inter dependent variables a proper understanding of the role of substantial physical variables and of their conditional grouping to cover the widely different fluid flow and speed regimes are necessitated. A space vehicle during its acceleration not only faces the changes in rarefaction (continuum, slip, transitional and free flow) when it crosses the different bounds of the atmosphere, but with the change in speed or change in Mach Number, complexity due to different levels of compressibility unique to the each of the flight flow regimes (subsonic-incompressible, subsonic-compressible, transonic, supersonic and hypersonic) adds another dimension to the prediction of thermal effects.

The problem becomes more significant at higher altitudes due to the variation of properties associated with high velocities at high altitude. Under these circumstances factors such as entropy layer, viscous interaction, high temperature, low density and real gas effects must be considered while simulating the flow. For example at high velocity the boundary layer becomes thick due to high kinetic energy dissipation within the boundary layer causing an increase in viscosity and temperature and decrease in density. This thickening of boundary layer introduces a viscous inviscid interaction causing problems for the boundary layer

analysis which effects the surface pressure distribution. Analysis[1] show that even at low supersonic speeds this viscous-inviscid interaction has significant effect on pressure distribution. Although efforts have been made to treat these type of problems by treating the boundary layer and the inviscid part separately, but this is still an approximation. Boundary layer also fails in case viscous/inviscid flow fully merges or if the vortices are present in the flow. An obvious choice to solve such strong interactive flow is using Navier Stokes Equation.

Based on this strategy Navier Stokes Equations are applied to a cone representing the fore body of the V2 rocket. Since the flow is purely conical therefore Navier Stokes Equations in Locally conical form can be used. This will help reduce the computing resource and time, which is very critical when simulation is done at each point in time in space along the flight path.

This paper presents the equations and the numerical techniques used. Results through CFD are used to improvise the classical method. For validation and bench marking[2], telemetry results used for V2 rocket are used. The results provided are at 1.5 feet length and the skin factor value of 0.34.

3 Numerical Method & Solution Scheme

For the present case study, a reduced form of Navier Stokes with locally conical approximation is being used. The method uses the three-dimensional unsteady compressible Navier Stokes equation in a spherical coordinate system. It is based on the assumption that for high-speed flow the gradients are much smaller in the radial than that in cross flow direction. Navier Stokes Equation under this locally conical approximation can then be derived in non dimensionalized form as ^[3]

$$\frac{\partial U}{\partial t} + \frac{\partial F}{\partial \theta} + \frac{\partial G}{\partial \phi} + H = 0 \quad (1)$$

where

$$U = \sin \theta \begin{bmatrix} \rho \\ \rho u_r \\ \rho u_\theta \\ \rho u_\phi \\ \rho e \end{bmatrix} \quad (2)$$

$$F = \sin \theta \begin{bmatrix} \rho u_\theta \\ \rho u_r u_\theta - \tau_{r\theta} \\ \rho u_\theta^2 + p - \tau_{\theta\theta} \\ \rho u_\theta u_\phi - \tau_{\phi\theta} \\ (\rho e + p)u_\theta + q_\theta - u_r \tau_{r\theta} - u_\theta \tau_{\theta\theta} - u_\phi \tau_{\phi\theta} \end{bmatrix} \quad (3)$$

$$G = \begin{bmatrix} \rho u_\phi \\ \rho u_r u_\phi - \tau_{r\phi} \\ \rho u_\theta u_\phi - \tau_{\theta\phi} \\ \rho u_\phi^2 + p - \tau_{\phi\phi} \\ (\rho e + p)u_\phi + q_\phi - u_r \tau_{r\phi} - u_\theta \tau_{\theta\phi} - u_\phi \tau_{\phi\phi} \end{bmatrix} \quad (4)$$

$$H = \sin \theta \begin{bmatrix} 2\rho u_r \\ 2\rho u_r^2 - \rho u_\theta^2 - \rho u_\phi^2 - \tau_{rr} + \tau_{\theta\theta} + \tau_{\phi\phi} \\ 3\rho u_r u_\theta - \text{ctg}\theta(\rho u_\phi^2 + p) + \text{ctg}\theta\tau_{\phi\phi} - 2\tau_{r\theta} \\ 3\rho u_r u_\phi - \text{ctg}\theta\rho u_\theta u_\phi - \text{ctg}\theta\tau_{\theta\phi} - 2\tau_{r\phi} \\ 2u_r(\rho e + p) - u_r \tau_{rr} - u_\theta \tau_{r\theta} - u_\phi \tau_{r\phi} \end{bmatrix} \quad (5)$$

Where shear stress terms are as follows

$$\begin{aligned} \tau_{rr} &= -\frac{2}{3\text{Re}_{\infty,r}}(2u_r + \frac{\partial u_\theta}{\partial \theta} + \text{ctg}\theta u_\theta + \frac{1}{\sin \theta} \frac{\partial u_\phi}{\partial \phi}) \\ \tau_{\theta\theta} &= \frac{2\mu}{\text{Re}_{\infty,r}}(\frac{\partial u_\theta}{\partial \theta} + u_r) + \tau_{rr} \\ \tau_{\phi\phi} &= \frac{2\mu}{\text{Re}_{\infty,r}}(\frac{1}{\sin \theta} \frac{\partial u_\phi}{\partial \phi} + u_r + u_\theta \text{ctg}\theta) + \tau_{rr} \\ \tau_{r\theta} = \tau_{\theta r} &= \frac{\mu}{\text{Re}_{\infty,r}}(-u_\theta + \frac{\partial u_r}{\partial \theta}) \\ \tau_{\phi\theta} = \tau_{\theta\phi} &= \frac{\mu}{\text{Re}_{\infty,r}}(\frac{\partial u_\phi}{\partial \theta} - \text{ctg}\theta u_\phi + \frac{1}{\sin \theta} \frac{\partial u_\theta}{\partial \phi}) \\ \tau_{r\phi} = \tau_{\phi r} &= \frac{\mu}{\text{Re}_{\infty,r}}(\frac{1}{\sin \theta} \frac{\partial u_r}{\partial \phi} - u_\phi) \end{aligned} \quad (6)$$

and heat flux is defined as

$$q_\theta = \frac{-\mu}{2\text{Re}_{\infty,r}} \frac{\partial T}{\partial \theta}$$

$$q_\phi = \frac{-\mu}{2\sin \theta \text{Re}_{\infty,r}} \frac{\partial T}{\partial \phi} \quad (7)$$

The viscosity has been calculated by using the Sutherlands law.

For the solution a time marching MacCormack two-step implicit finite difference method scheme is employed using the following predictor and corrector to the equation (1).

Predictor:

$$\begin{aligned} \Delta U_{i,j}^n &= -\Delta t(\Delta_+ \frac{F_{i,j}^n}{\Delta \theta} + \Delta_+ \frac{G_{i,j}^n}{\Delta \phi} + H_{i,j}^n) \\ [I - (\frac{\Delta t}{\Delta \theta})\Delta_+ |A^n|][I - \frac{\Delta T}{\Delta \phi} \Delta_+ |B^n|] \delta U_{i,j}^{n+1} \end{aligned} \quad (8)$$

$$U_{i,j}^{n+1} = U_{i,j}^n + \delta U_{i,j}^{n+1}$$

Corrector

$$\begin{aligned} \Delta U_{i,j}^{n+1} &= -\Delta t(\Delta_- \frac{F_{i,j}^{n+1}}{\Delta \theta} + \Delta_- \frac{G_{i,j}^{n+1}}{\Delta \phi} + H_{i,j}^{n+1}) \\ [I - (\frac{\Delta t}{\Delta \theta})\Delta_- |A^{n+1}|][I + \frac{\Delta T}{\Delta \phi} \Delta_- |B^{n+1}|] \delta U_{i,j}^{n+1} \\ U_{i,j}^{n+1} &= (U_{i,j}^n + U_{i,j}^{n+1} + \delta U_{i,j}^{n+1}) \frac{1}{2} \end{aligned} \quad (9)$$

where $|A|$ & $|B|$ are matrices with positive eigen values.

Although shock waves are captured automatically through this procedure, the oscillations in the flow parameters are very high near the shock waves due to discontinuities at the shock wave for compressible flow. Therefore to dampen these oscillations modified adaptive artificial viscosity term (AAV) is applied in a conservative style. This term is significant to the calculation near the shock wave. It has very little effect inside the boundary layer. It has also been observed that for an accurate viscous solution, the AAV must be switched off near the wall; otherwise residues near wall cannot be reduced further after two orders of reduction have been achieved.

Numerical solution gives fluid properties of temperature, pressure, velocity, density and Mach number on a computation surface at a distance 'r' from the tip, as shown in fig.1.

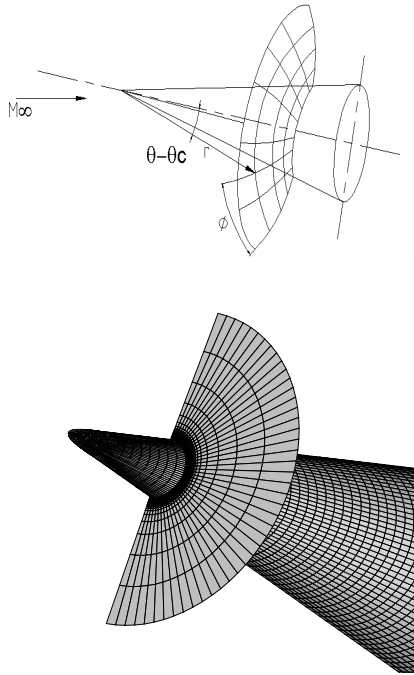


Fig.1. Computation Surface

4 Model Geometry and Flow Conditions

An equivalent cone of 13 degree half angle representing the nose part of the V2 rocket is used for simulation. Position of the station for which simulation is being carried out is at 1.5 feet from the apex. This is the position where the gauges are placed during the telemetry.

To compute the temperature and other flow parameters under the actual transient high-speed variable altitude flight conditions, require the free stream conditions all along the flight path. Trajectory data along the flight path at one-second interval was generated and free stream conditions for each step were then created using standard atmospheric model to be used as input to numerical simulation.

Position for the computed station is located through Reynolds number.

Although for very high Mach numbers and high temperatures molecules may dissociate

but for the present case trajectory chosen is such that a perfect gas can be assumed. Therefore,

$$P = \rho RT$$

$T = (\gamma - 1) [e - (v)^2/2] R$ with the gas constant, $R = 287 \text{ m}^2/\text{sec}^2\text{K}$ and $\gamma = 1.4$.

For boundary conditions all three velocity vectors are assumed zero on the body surface with $T = T_w = \text{Constant}$. At the outer boundary free stream conditions and on the symmetric planes reflection conditions are assumed.

5 Grid

A grid of 65x65, as shown in fig.2 is being used for numerical simulation. Grid is evenly distributed along the circumferential direction ϕ and stretched in the θ direction towards the wall to resolve the viscous effects.

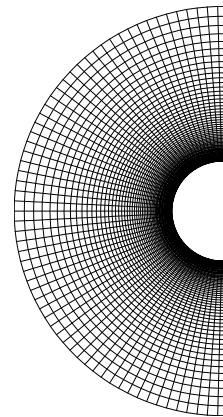


Fig.2. Computational Grid

6 Results and Discussion

Determining the temperature for a given body geometry or skin under the actual transient high speed variable altitude flight conditions is a very lengthy step by step process. When investigating the interdependence of main physical parameters takes a different form in each of four flow regimes. To find out the local thermal values an appropriate integration procedure at any given time instant (t), during a

generally transient flight history of any vehicle require an iterative process which determine flow regimes (Kn) and its dependence on actual local skin temp conditions due to the kind of boundary layer present, Mach number and Re number. It also requires a suitable functional representation of all other local physical or dimensionless parameters ($\gamma, \alpha, k, \mu, M, \rho_0, P, Pr$ etc.) in terms of local transient skin temperature values.

To cater for this complexity a useful grouping can be done on the basis of defining a relationship between Kn, M and Re Number. A lower and upper bound can then be defined to be used as input to find out the local flow type/ flow conditions for the given vehicle at a given point on its trajectory. At any successive time skin temperature believe to be the function of all the previous time history of their variations, from initial conditions up to the investigating moments. Table 1 shows criteria of grouping for different flow regimes.

Discretization of Flow Regimes	
CONTINUUM FLOW	$Re \gg 1,$ $0 < M < 15$ Upper bound: $Kn_L = \lambda / L \sim M / (Re_L) < < 1$ Lower bound : $Kn_\delta = \lambda / \delta \sim M / \sqrt{Re_L} < 0.01$
TRANSITION FLOW	Upper bound: $Kn = \lambda / L \sim M / (Re_L) < 3$ Lower bound : $Kn = \lambda / \delta \sim M / \sqrt{Re_L} > 0.1$
SLIP FLOW	$Re_L > 1,$ $M > 1$ $1e-2 < Kn = \lambda / \delta \sim M / \sqrt{Re_L} > 0.1$
FREE MOLECULAR FLOW	$Re \sim 0$ $Kn_\delta =$ Does not exist $Kn_L = \lambda / L \sim M / (Re_L) > 3$

Table 1: A Criterion for Various Flow Regimes.

For skin temperature calculation ^{[2][4]} a heat balance equation is used. It is based on assumptions, that total heat required to raise the temperature of a body is sum of convection, radiation and solar term. It is also assumed that no conduction or radiation takes place to the

structure. All the methods described next take its basis from this heat balance equation, which is a non-linear differential equation to be solved through integration by numerical methods. In equation form

$$\frac{dT_s}{dt} = \frac{h(T_B - T_s) + \epsilon\sigma(\delta T_A^4 - T_s^4) + \epsilon C}{c\tau w} \quad (10)$$

Or

$$(c\tau w) \frac{dT_s}{dt} = h(T_B - T_s) + X$$

Where $X = \frac{\epsilon\sigma(\delta T_A^4 - T_s^4) + \epsilon C}{c\tau w}$

Another way of writing the same equation is ^[4]

$$(c\tau w) \dot{T}_w = h_{cp}(H_B - H_s) + X \quad (11)$$

Where $H = C_p \Delta T$

The solution for this equation can be written as ^[2]

$$T_s = (T_p - BT_m^4)(1 - e^{-\Delta t/\theta}) + T_i e^{-\Delta t/\theta} \quad (12)$$

Authors should recognize the possibility for full colour publishing of photographs and illustrations. Image files should be optimized to minimize size without compromising the quality. The figures should have a resolution of 300 dpi.

6.1 Method I

To solve the above equation Webber^[2] takes its foundation from the Newtonian theory ^[5]. Boundary layer temperatures are achieved using stagnation temperature and the free stream temperature with an interrelation of recovery factor. The recovery factor has been assumed to be equal to square root of Prandtl number.

$$T_B = T_A + k(T_T - T_A)$$

For calculation a perfect gas with laminar flow has been assumed. Heat transfer coefficient h is calculated by using Nusselt number, thermal conductivity and characteristic relation

$$h = N_u \cdot k / L$$

Where $N_u = (.0071 + .0154 \beta^{0.5}) Re^{0.8}$ and μ, k values are based on values from gas tables^[6]. Above Nu Number relationship is based on experimental results from wind-tunnel.

Viscosity has been calculated both at boundary layer temperature (T_B) and the surface temperature (T_S). Results of method I has been listed in table 2, and in fig.3 and fig.4.

An extension of this method is developed by Quinn^[2]. In his method heat transfer coefficient has been calculated for a flat plate and then correction has been made for the wedge and cones using free stream conditions. Although heat transfer coefficient has been calculated by using enthalpies, final solution does employ the boundary layer temperature as employed in method I.

Using the appropriate editor each equation should occur on a new line with uniform spacing from adjacent text as indicated in this template. The equations, where they are referred to in the text, should be numbered sequentially and their identifier enclosed in parenthesis, right justified. The symbols, where referred to in the text, should be italicized.

6.2 Method II

Method II is based on the approach explained in this paper and effort has been made to overcome some of the assumptions described in the earlier two methods. In this paper an approach has been used where the part of corrections etc to be made due to axysymmetric flow, shape factor, viscous effects, shock layer boundary layer interaction etc comes as part of the numerical solution. Numerical solution has been sought through solving Navier Stokes with conical assumptions at each second's interval.

Free stream values for simulation are changed at every interval according to the vehicle location in the atmosphere and its speed. Flow parameters across the shock are then used to upgrade the skin temperature using reference enthalpy method. This confirms that reference temperature or enthalpy can be directly related to an average temperature or enthalpy obtained from numerical solutions.

Results are compared in table.2 and fig.5 for both methods. Results show that current method gives only 5 to 10 % error from telemetry data at different altitudes during flight. This can be attributed to change in C_p , gamma and Prandtl Number, which are kept constant during numerical simulation. Another reason for variation from telemetry could changes in attitude and angles of attack during actual flight. Temperature sensors during some of the flight time remain towards low temperature or low pressure region. It can be seen from fig.6a to fig.6c that temperature inside the boundary layer increases as we increase the angle of attack from 4° to 16° . Whereas for the present study it has been assumed that temperature sensors are placed towards high α during the whole flight envelop. In addition a $\pm 10\%$ error in the telemetry data has also been mentioned.

7 Conclusion

Following conclusions can be drawn from this study

- Using the free stream Reynolds number and the Mach number one can roughly estimate the flow conditions and behavior of the air but using the criteria shown in Table 1 it can be seen that the assumption of a calorically perfect gas seems obscured. It gives satisfactory approximation for which the high supersonic flight remains in a particular domain.
- Also, most of the theories developed in this context for approximation are based on continuum flow with small angle of attack but in actual AOA may go very high thus adding difficulty in terms of modeling the flow through classical methods. Even for angle of attacks, alpha 4 to 16 deg, flow's behaviour over a cone shows development of separation and local hot points which can only be modeled through Navier Stokes. Thus using such

approach, all the complexity in flow phenomenon due to change in M , α or altitude will come as part of the solution (fig 6a-6c). This will lead to more accuracy in terms of heat prediction at any local point on the body.

- For the trajectory of V2 rocket considered above, approximation of perfect gas may be valid because of the limiting temperature involved and flight envelop considered, but in actual for long trajectories real gas effects must be incorporated during simulation.

8 References

- [1] Chaudhry S R, Qin N and Richards B E. Hypersonic viscous flow around waverider configurations. Paper presented at *1st Hypersonic waverider Symposium*, University of Maryland, USA. Oct 17-19, 1990.
- [2] Huston W B. Study of skin temperatures of conical bodies in supersonic flight. (*NACA TN 1724*), 1947.
- [3] Anderson D A, Tannehill J C and Pletcher R H. *Computational fluid mechanics and heat transfer*. 2nd edition, Taylor & Francis, pp 479-480, 1997.
- [4] Quinn R D. Real time aerodynamic heating and surface temperature calculations for hypersonic flight simulation. (*NASA TM 4222*), Aug 1990.
- [5] Anderson J D. *Hypersonic and high temperature gas dynamics*. AIAA Publication, pp 66-70, 1999.
- [6] Hanson F. Approximations for the thermodynamic and transport properties of high temperature air. (*NACA TN 4150*), pp 55, Mar 1958.

Data extract for Aluminum section at 1.5 ft(V2)				
Time Sec	Al surface Temp Celsius (Method 1 using T_g)	Al surface Temp Celsius (Method 1 using T_g)	Al surface Temp Celsius (Method 2 based on CFD)	Al surface Temp Celsius (Telemetry data)
1	22.03	22.03	-	22
10	20.86	20.87	-	22
15	19.80	19.81	-	22
20	19.34	19.35	-	22
25	20.55	20.57	-	22
30	24.19	24.23	26.55	22
35	30.41	30.53	30.92	35
40	39.82	40.13	39.50	45
45	55.51	56.45	55.32	62
50	77.35	79.69	79.56	87
55	100.13	104.45	106.89	108
60	119.83	126.37	133.19	124
65	133.09	141.38	151.99	135
70	139.40	148.55	166.26	142
75	141.79	151.24	169.51	147
80	142.90	152.46	170.96	156
100	143.56	153.10	-	160

Table 2: Comparison of Telemetry Data with Computational Data.

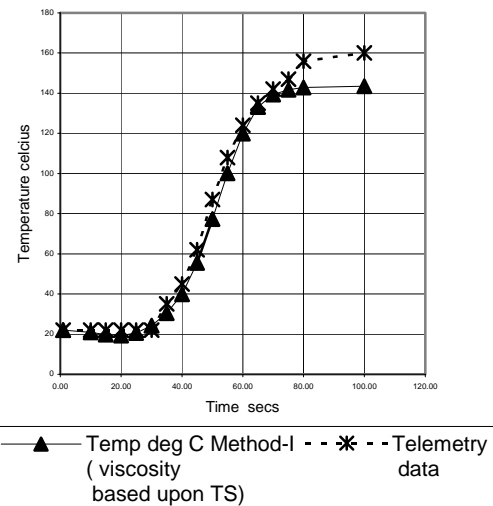


Fig. 3. Skin Temperature for V2 using Method 1 based on (TS)

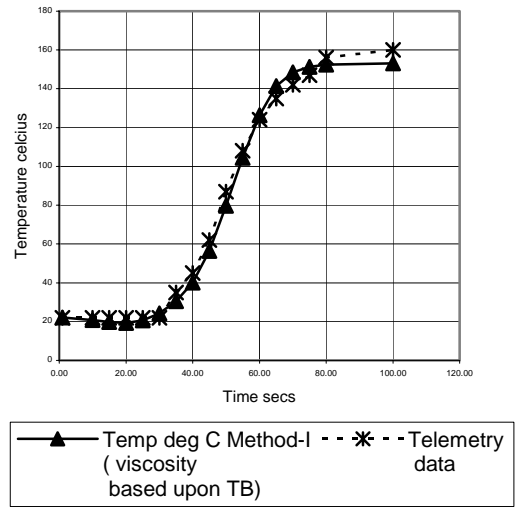


Fig. 4. Skin Temperature for V2 using method-I Based on (TB)

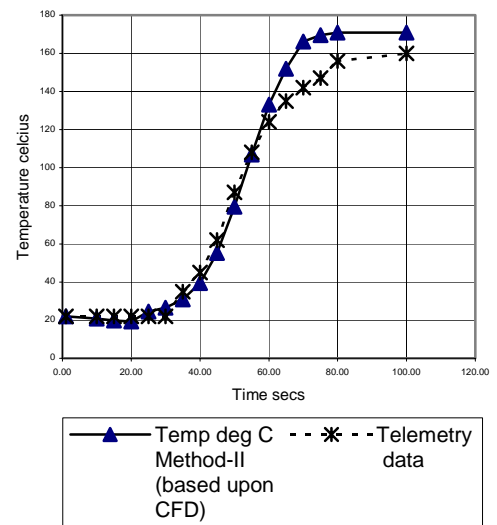


Fig. 5. Skin Temperature for V2 using CFD

ESTIMATION OF SKIN SURFACE TEMPERATURE OF SPACE VEHICLES DURING WHOLE FLIGHT ENVELOPE

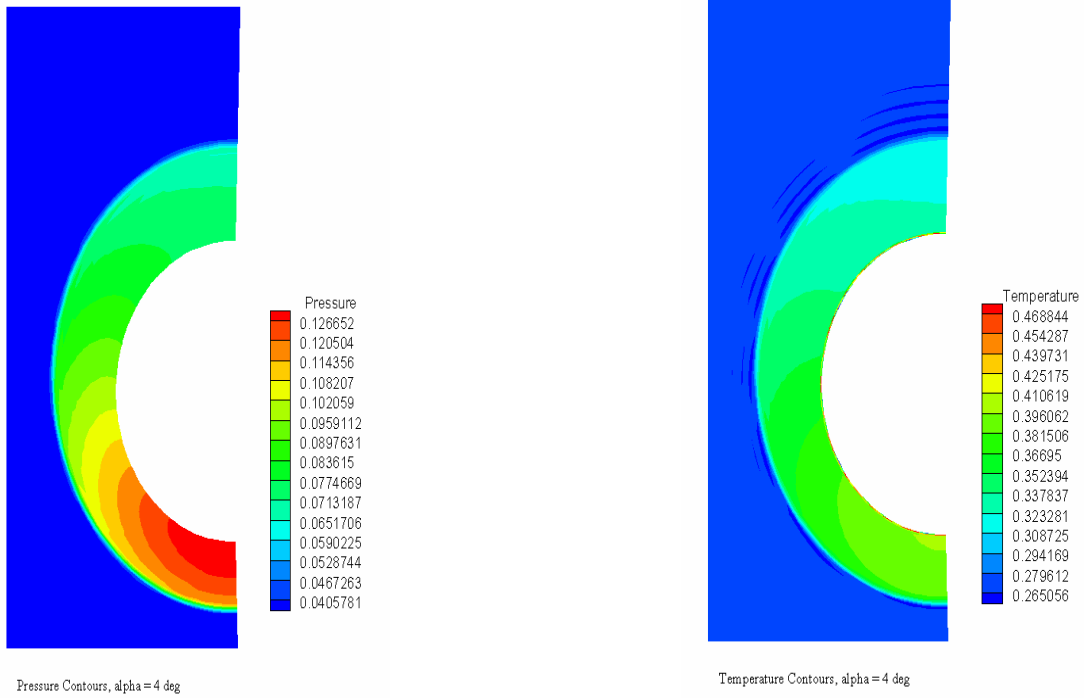


Fig. 6a. Flow Field Contours for 13 Degree Cone, Mach # = 4.3348, Re # = 8.722e05, Alt = 29km, $\alpha = 4^\circ$

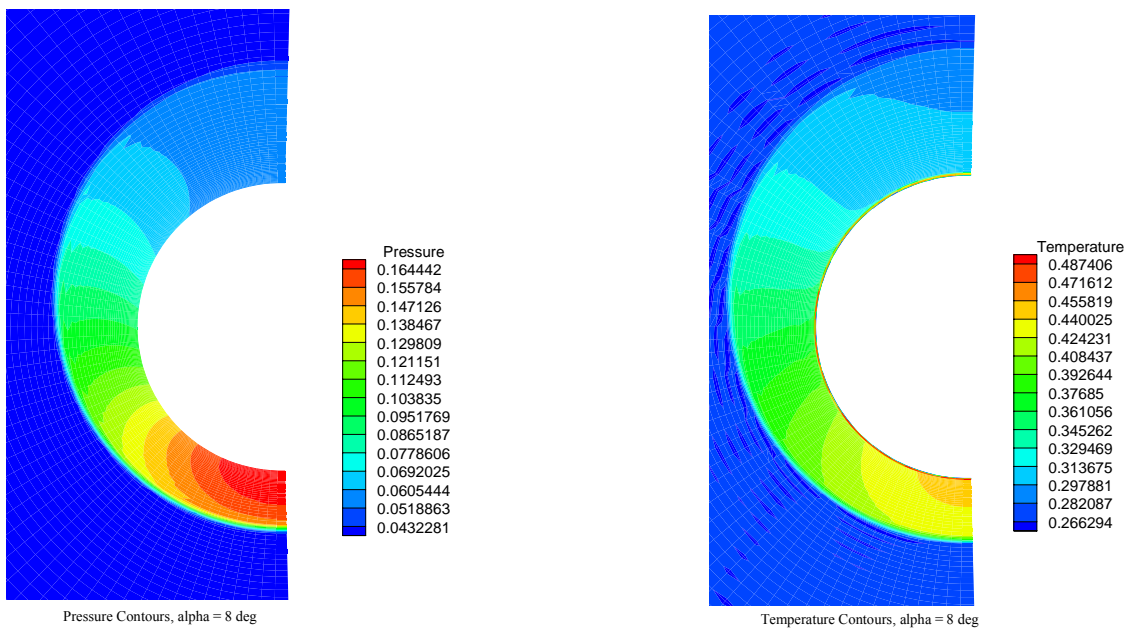


Fig. 6b. Flow Field Contours for 13 degree cone, Mach # = 4.3348, Re # = 8.722e05, Alt = 29km, $\alpha = 8^\circ$

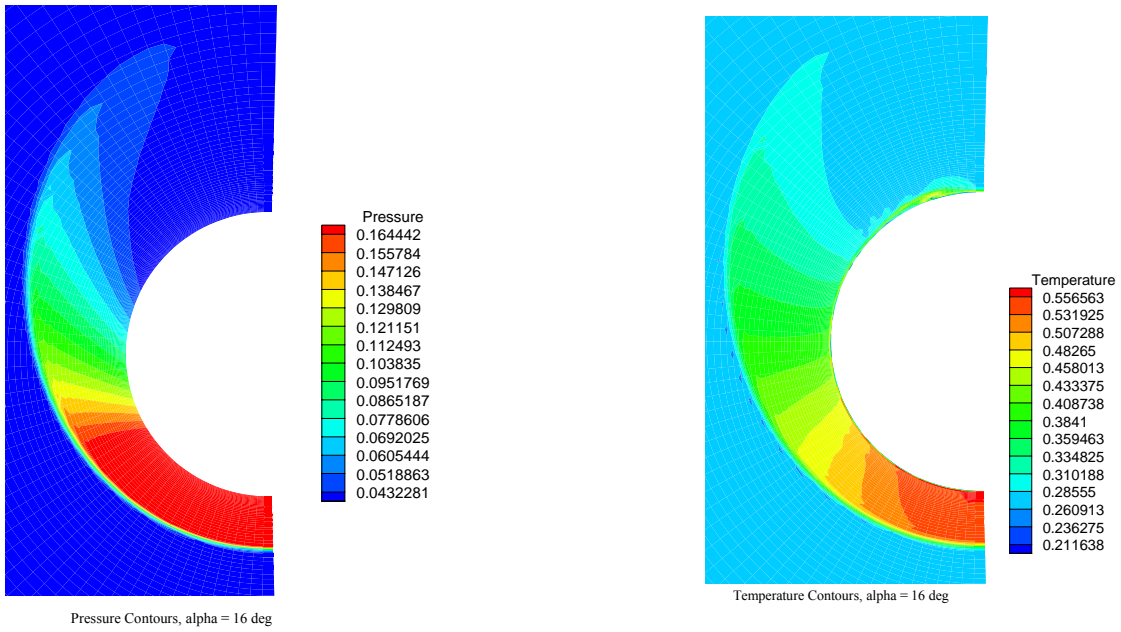


Fig. 6c. Flow Field Contours for 13 degree Cone, Mach # = 4.3348, Re # = 8.722e05, Alt = 29km, $\alpha = 16^\circ$